Fluidisation of Mud by Waves

Development of a mathematical model of fluid mud in the coastal zone

W Roberts

Report SR 296
February 1992

HR Wallingford

Registered Office: HR Wallingford Ltd, Howbery Park, Wallingford, Oxfordshire OX10 8BA, UK
Telephone: 0491 35381 International + 44 491 35381 Telex: 848552 HRSWAL G.
Facsimile: 0491 32233 International + 44 491 32233 Registered in England No. 1622174

Contract

This report describes work funded by the Department of the Environment under Research Contract PECD 7/6/143 for which the nominated officer was Mr P Woodhead and by HR Wallingford. The HR job number was UQS 59. It is published on behalf of the Department of the Environment, but any opinions expressed in this report are not necessarily those of the Department of the Environment. The report was written by W Roberts in Dr A J Cooper's section of the Research Department, headed by Dr W R White. The project was managed by M C Ockenden.

Prepared by William Roberts MATHEMATICAL MODELLER

Checked by A J Cooper SECTION MANAGER

Approved by M. C. Ockenden PROJECT MANAGER

Date 16.6.92

Summary

Fluidisation of Mud by Waves

Development of a mathematical model of fluid mud in the coastal zone

W Roberts

Report SR 296
February 1992

A mathematical model of mud transport in the coastal zone has been developed, which simulates the movement of suspended and fluid mud in response to the action of waves and tidal currents. It is based on existing HR Wallingford models of mud transport but incorporates the novel features of fluidisation of a muddy bed by the action of waves and a multi-layer representation of the bed consolidation process. The new model represents the interchange of mud between its three phases: settled mud on the bed, fluid mud and suspended mud. Once formed, either by fluidisation of the bed or by hindered settling, the fluid mud may move under the influence of gravitational and hydrostatic forces and currents in the overlying water. The movement of fluid mud is assumed to have a negligible feedback effect on the motion of the overlying water.

The high level of wave activity during a storm can mobilise very large quantities of sediment in the form of fluid mud, which can then flow into navigation channels and berths. Subsequent dewatering can lead to high levels of siltation, far above what could be expected from settlement of suspended mud alone.

As a test, the model is used to simulate the effects of a storm on patterns of erosion and deposition in Tees Bay. The initial conditions for the bed deposits were not intended to be realistic, but rather to make a substantial amount of sediment available for erosion. Large areas of the bed were observed to be fluidised during the storm and fluid mud flowed into a dredged navigation channel causing a high degree of siltation.

It is noted that the model could be improved by further work on the turbulent entrainment of fluid mud into the overlying water.

Contents

Contents (Continued)

1 Introduction

This report describes the development of a model of mud transport in coastal areas. Most previous research has concentrated on the effect of tidal currents on erosion and deposition of mud; the model described here also takes into account the effect of waves on mud erosion, in particular the phenomenon of fluidisation of a soft muddy bed by the action of waves. The aim of the work was to develop a model which would use the results of laboratory and field work on fluidisation of mud by waves, carried out at HR Wallingford on behalf of the Department of the Environment (Ref 1). Using this model, it was possible to assess the effects of the fluidisation phenomenon in a coastal environment, where the influence of factors such as tidal water levels and currents and sea bed bathymetry is important.

Fluid mud is a dense suspension containing a concentration of mud flocs which is high enough to cause a significant change in the physical properties of the mud-water mixture when compared to those of clear water. Once a fluid mud layer has been formed it can flow under the influence of gravity, hydrostatic pressure gradients (caused by the slope of the water surface or the slope of the fluid mud-water interface) and the overlying water currents. In some circumstances this process can make a major contribution to the pattern of mud transport.

The model development draws on previous work on fluid mud by Odd and Rodger (Ref 2) and Odd & Cooper (Ref 3) and on the existing HR model MUDFLOW-2D. In Chapter 2, the structure and basic assumptions of the model are described and other related work is reviewed. The equations governing the formation and movement of fluid mud, the transport of mud in suspension and the behaviour of bed deposits are set out in Chapter 3. Chapter 4 describes the numerical scheme used to implement these equations and the application of the model to a test case is detailed in Chapter 5.

2 Basis for the model

2.1 Fluid mud properties

There are two main ways in which a layer of fluid mud can form: by hindered settling and by fluidisation of the bed by wave-induced stresses. Previous models of fluid mud at HR (Ref 3) have included only the first of these processes, in which mud settles from suspension more rapidly than it can dewater, hence forming a layer of fluid mud. This occurs at slack water in many turbid tidal estuaries, for instance the Severn. The model described in this report also takes into account the way in which the action of waves can break up the structure of a soft muddy bed, through oscillatory shear stresses and wave-induced pressure gradients. This process is described in more detail by Ross and Mehta (Ref 4), who note that a layer of fluid mud is characterised by an effective stress (the difference between the total vertical stress and the pore water pressure) of approximately zero and that the density in the fluid mud layer may be the same as in the upper part of the muddy bed. Once fluidised in this way, the level of the mud-water interface is determined by a balance between upward turbulent diffusion and the negative buoyancy of the dense fluid mud. It is assumed in the model that this interface will coincide with the top of the wave boundary layer, as the wave boundary layer is associated with a high intensity of turbulence. It is possible that a sufficiently large amount of mud may be fluidised for the level of the interface to be governed by hindered settling with the fluid mud extending upward beyond the depth of the wave boundary layer.

The complex interaction between fluid mud and the turbulent flow beneath a wave is not fully understood and the model described here necessarily represents it in a simplified way, partly because of the many unknown factors and partly because this process is only one element of a more general hydraulic model which is subject to the practical limitation of reasonable execution time on the available computers. One example of this is the way in which the strength of the bed is represented: the resistance of the bed to fluidisation by waves is parametrised in the model in terms of the critical shear stress for erosion, which deals essentially with particulate erosion from the surface of the bed. While this certainly plays a part in the formation of fluid mud, Jiang and Mehta (Ref 5) document field measurements of fluid mud layers under waves which are too small to cause particulate erosion. The laboratory experiments carried out as the first part of this research project (Ref 1) have shown that the process of fluidisation is extremely complex, being strongly influenced by the structure of the mud bed and the frequency spectrum, as well as the height and period, of the applied waves. The structure of the bed depends on a large number of interacting factors including the particle size, mineralogy, chemical composition, ionic strength and local stress history. Therefore, in this pilot mathematical model, we aim to represent only the most important features of bed fluidisation.

It is assumed that fluid mud is a viscous Newtonian fluid. Field measurements of mud from the River Parrett confirm that this is a more accurate representation than treating the fluid mud as a Bingham fluid, as in previous work at HR (Refs 3,6). The viscosity is assumed to be a function of the mud concentration. Jiang and Mehta (Ref 5) agree that fluid mud is a Newtonian fluid at moderate to high shear rates but at low shear rates they describe it as pseudoplastic.

2.2 Model structure

The model consists of three parts: a dilute suspension of mud, a fluid mud layer and a muddy bed, which is divided into a number of layers in order to represent the way in which the density and erosion strength of a consolidated mud bed increase with depth. The transport of mud in suspension is modelled exactly as in MUDFLOW-2D: by solving the advection-diffusion equation for the mud concentration (equation (1)), where the water depth and discharge have been calculated previously and stored. Thus the coupling between the mud concentration and the flow is assumed to be small and is neglected. The motion of the fluid mud is determined by solving a restricted form of the shallow water equations. The mass conservation equation (equation (2)) is as usual, but in the momentum equations (equations (3) and (9)) the non-linear and diffusion terms are assumed small and discarded.

The bed is represented by a number of layers, each associated with a particular average dry density and characterised by an erosion shear strength and a yield strength. The erosion shear strength of a particular layer is the minimum stress required to cause erosion of mud of that density. The yield strength is a way of characterising the resistance of mud to vertical stresses. For a particular layer, it is defined as the mass of mud per m^2 above the base of that layer when the bed has reached its equilibrium density-depth profile, thus representing the maximum weight which can be supported by mud of that density. The units are kg/m^2 which corresponds to a stress divided by the gravitational constant. It is determined from the equilibrium density-depth profile of the bed which is found from laboratory studies of the mud from the location to be modelled. When mud is deposited onto the bed, it is added to the top, lowest density layer. At each time-step, the total mass of mud above the base of each layer is compared to the yield strength of that layer, and if there is an excess, some proportion of the excess is transferred to the denser, stronger layer below. In this way the process of consolidation is represented, and the rate of consolidation is governed by the proportion of the excess mud which is transferred at each time-step. The erosion process always removes mud from the uppermost occupied bed layer, but as erosion continues, the lower density layers may be completely removed, exposing stronger mud at the bed surface. The total amount of mud available for erosion is thus limited.

An important aspect of the model is the exchange of mud between the bed, the fluid mud and suspension. These are summarised in figure 1. In the absence of fluid mud, mud can be exchanged directly between the bed and suspension by settling and erosion. Settling can occur only if the shear stress at the interface is below the critical stress for deposition and erosion occurs only when the stress is greater than the critical stress for erosion of the exposed bed layer. The shear stress is related to the intensity of the turbulence. When fluid mud is present, similar processes occur, but now there are two interfaces to consider, rather than just one. Mass can be transferred to the bed by dewatering and, if the fluid mud is moving sufficiently quickly, it can erode mud from the bed. These processes are associated with the same critical stresses as those for exchange between mud in suspension and the bed. Note that the presence of waves can cause erosion of the bed, with or without the presence of fluid mud, by enhancing the stress at the bed. Mud can settle from suspension onto the fluid mud. Mass transfer from the fluid mud into suspension can occur either by particulate erosion from the interface, or by turbulent entrainment. Entrainment can occur only at low values of the bulk Richardson number, which represents the relative importance of the density gradient and the intensity of the turbulence. At higher values of the Richardson number, the turbulence of the flow is insufficient to overcome the negative buoyancy of the fluid mud. The physical processes involved in entrainment are discussed by Fernando and Stephenson (Ref 7), who suggest two primary mixing mechanisms: Kelvin-Helmholtz instabilities and breaking or instability of interfacial waves. The equations governing the rates of these various exchanges are given in the next chapter.

3 Governing equations

3.1 Transport suspended mud

The transport of suspended mud is modelled by the advection-diffusion equation:

$$\frac{\partial c}{\partial t} + \frac{u\partial c}{\partial y} + \frac{v\partial c}{\partial y} = \frac{1}{d}\left\{\frac{dm}{dt} + \frac{\partial}{\partial x}\left(dD_x\frac{\partial c}{\partial x}\right) + \frac{\partial}{\partial y}\left(dD_y\frac{\partial c}{\partial y}\right)\right\}, \tag{1}$$

where c is the concentration averaged over the water depth (kg/m^3), d is the water depth (m), u and v are components of water velocity (m/s), also depth-averaged, and dm/dt is the net rate of mass exchange of mud (kg/m^2/s). The contributions to the net mud exchange are detailed below. D_x and D_y are eddy diffusivities.

3.2 Fluid mud flow

The conservation of mass of fluid mud is expressed as:

$$\partial\frac{(c_m d_m)}{\partial t} + \frac{\partial}{\partial x}(u_m d_m c_m) + \frac{\partial}{\partial y}(v_m d_m c_m) = \frac{dm}{dt}, \tag{2}$$

where c_m is the concentration of the fluid mud (kg/m^3), d_m is the depth of the fluid mud layer, u_m and v_m are depth-averaged fluid mud velocity components and dm/dt is the net rate of mass exchange as in the advection-diffusion equation.

The equation of motion in the x-direction is given by:

$$\frac{\partial u_m}{\partial t} + \frac{1}{d_m\rho_m}(\tau_o - \tau_i)_x - \Omega v + \frac{\rho_w}{\rho_m} g \frac{\partial\eta}{\partial x}$$
$$+ g\frac{\Delta\rho}{\rho_m}\frac{\partial\eta_m}{\partial x} + \frac{gd_m}{2}\frac{\partial\Delta\rho}{\partial x} = 0, \tag{3}$$

where

$$\rho_m = \rho_w + \Delta_\rho \tag{4}$$

and

$$\Delta\rho = 0.62\ C_m \tag{5}$$

ρ_m is the density of fluid mud, ρ_w is the density of the overlying water, assumed to be constant, and η and η_m are the elevations of the water surface and the mud-water interface respectively. Ω is the Coriolis parameter (s^{-1}), τ_o is the shear stress at the bed (N/m^2), discussed in the next section, and τ_i is the shear stress at the interface (N/m^2) given by

$$\tau_i = \frac{1}{8} f\rho(\Delta u^2 + \Delta v^2), \tag{6}$$

where

$$\Delta u = u - u_m \tag{7}$$

and

$$\Delta v = v - v_m \tag{8}$$

and f is a friction factor.

The non-linear terms and the diffusion terms have been assumed to be small in comparison with the other terms and variations in the density have been included only where they give rise to a buoyancy force (the Boussinesq approximation).

The equation in the y-direction is similar:

$$\begin{aligned} &\frac{\partial v_m}{\partial t} + \frac{1}{d_m \rho_m}(\tau_o - \tau_i)_y + \Omega u + \frac{\rho_w}{\rho_m} g \frac{\partial \eta}{\partial y} \\ &+ g \frac{\Delta\rho}{\rho_m}\frac{\partial \eta_m}{\partial y} + \frac{g d_m}{2}\frac{\partial \Delta\rho}{\partial y} = 0 \end{aligned} \tag{9}$$

3.3 Bed stress under a fluid mud layer

The bed stress due to a moving fluid mud layer is calculated from a curve fitted to an analytical result relating a friction factor to the Reynolds number. The analytical work, described in detail by HR Wallingford (Ref 6), uses the depth averaged fluid mud velocity and the assumption that the fluid mud is a turbulent boundary layer to calculate the friction velocity at the bed. This can then be adapted to relate two dimensionless quantities, the friction factor and the Reynolds number. The result used in this model is:

$$\tau_o = \frac{1}{8} \rho_m f_m (u_m^2 + v_m^2), \tag{10}$$

where the friction factor is given by:

$$f_m = \begin{cases} 10^{(-\log R + 1.3802)} & if\ 0 \le R \le 46 \\ 1.506 \times 10^6 \times (0.01 \times 10^{(\log R)^{-0.88}})^{4.74} & if\ 46 < R \le 1200 \\ 460 \times (0.05 \times 10^{(\log R)^{1.23}})^4 & if\ 1200 < R \end{cases} \tag{11}$$

The Reynolds number is:

$$R = \frac{(U_m^2 + V_m^2)^{1/2} d_m}{\nu_m} \tag{12}$$

and the fluid mud viscosity, ν_m, is a function of concentration:

$$\nu_m(C_m) = 10^{-6} \, exp \, (\gamma C_m), \tag{13}$$

where

$$\gamma = \frac{1}{C_o} \ln \left(\frac{\gamma_m(C_o)}{10^{-6}} \right) \tag{14}$$

The exponential form of this equation is an assumption and the coefficients are chosen such that when $c=0$, the viscosity is that of clear water and when $c=c_0$, the viscosity is a known value determined from measurements. This value is an input parameter to the model and so can be adjusted for different muds. The increment to the bed stress caused by the presence of waves is given in section 3.5.

If the fluid mud layer is thicker than the wave boundary layer, it is assumed that the stress at the bed due to waves is attenuated by the presence of the fluid mud. In the absence of authoritative experimental or theoretical work on the subject, an ad hoc exponential relationship is assumed, whereby the stress is reduced by a factor of $1/e$ if the fluid mud layer extends to twice the thickness of the wave boundary layer.

3.4 Mud exchange between the bed, fluid mud and suspension

Mud is exchanged between states by the processes described in Chapter 2 and illustrated in Figure 1. Each of these exchanges represents a gain of mass by one state and a loss of mass by another, so whether the rate is positive or negative will depend on the context.

Settling of mud from suspension

Settling of mud from suspension is described by

$$\frac{dm}{dt} = V_s(c)c \left(1 - \frac{\tau}{\tau_d} \right) H \left[\tau_d - \tau \right], \tag{15}$$

where V_s is the settling velocity, which is a function of concentration c, τ_d is the critical shear stress for deposition, τ is the actual shear stress at the fluid mud-water interface or at the bed-water interface in the absence of fluid mud and H is the usual Heaviside step function

$$H(x) = \begin{cases} 1, & x > 0 \\ 0, & x \leq 0 \end{cases} \tag{16}$$

The settling velocity is given by:

$$V_s(c) = \begin{cases} V_{\min}, & c < \dfrac{V_{\min}}{R_o} \\ CR_o, & c \geq \dfrac{V_{\min}}{R_o} \end{cases} \tag{17}$$

where V_{min} is the minimum settling velocity (m/s) and R_0 is a constant (m^4/kg/s). As the concentration increases, more mud particles stick together to form larger heavier flocs which have a higher terminal velocity. V_{min} and R_0 are adjustable parameters of the model, determined by laboratory experiments on suitable mud samples.

Erosion

Erosion of mud from the bed by water or fluid mud and erosion of fluid mud by water are all governed by the same equation.

$$\frac{dm}{dt} = m_e(\tau - \tau_e)H[\tau - \tau_e] \tag{18}$$

where m_e is the erosion rate (kg/N/s), another constant parameter of the mud, τ_e is the critical shear stress for erosion (N/m^2) which depends on which layer of the bed or fluid mud is being eroded and is the actual shear stress at the appropriate interface.

Dewatering

Dewatering is the process by which fluid mud becomes a weak soil, modelled by transferring mud from the fluid mud layer to the lowest density bed layer at a rate given by:

$$\frac{dm}{dt} = V_o\, C_m\, H[10 - Ri_B] \tag{19}$$

where V_0 is the dewatering velocity (m/s) and c_m is the concentration of fluid mud (kg/m^3). τ_d is as above and τ is the shear stress at the fluid mud-bed interface. As with settling from suspension, dewatering can only occur at low shear stresses.

Entrainment

The rate at which mud is entrained from the fluid mud layer by the overlying water is given by:

$$\frac{dm}{dt} = V_e\, C_m\, H\left[10 - Ri_B\right], \tag{20}$$

where V_e is the entrainment velocity (m/s) given by:

$$V_e = \frac{0.1\ \Delta U}{(1 + 63Ri_B^2)^{3/4}}, \tag{21}$$

where

$$\Delta U = \left[(u - u_m)^2 + (v - v_m)^2\right]^{1/2}, \tag{22}$$

Entrainment can only occur at sufficiently low values of the bulk Richardson number. From experiment the critical value of Ri_B is chosen to be 10.

Consolidation of the bed

The way in which the consolidation process is modelled is explained in Chapter 2. The rate of mass transfer by consolidation from bed layer i to layer $i+1$ is given by

$$\frac{dm_i}{dt} = -A\left[\left(\sum_{j=1}^{i} m_j\right) - \zeta_i\right], \tag{23}$$

where m_j is the mass of mud per m^2 in layer j (kg/m^2) and ζ_i is the yield strength of layer i (kg/m^2), defined as the mass of mud per m^2 above the base of layer i when the bed has reached its equilibrium state. A is a consolidation rate constant. Solution of the above differential equation shows that the mass of mud at or below a given density, in excess of the value which corresponds to the equilibrium bed profile, will decrease by a factor

$exp(-A(t-t_0))$

in time $(t-t_0)$.

3.5 The effect of waves

The total stress at the bed in the presence of waves is the sum of a stress due to currents, the stress due to waves and a wave-current interaction term (Ref 8). The stress due to waves is calculated from the maximum wave orbital velocity at the bed, U_b, which must be calculated by a separate model (eg the HR PORTRAY model, Ref 9) and read in from file. It is related to the wave height and period and the water depth (Ref 10). The wave stress is calculated from

$$\tau_w = \tfrac{1}{2}\, \rho_w f_w U_b^2, \qquad (24)$$

where ρ_w is the density of clear water (kg/m^3) and f_w is the wave friction factor:

$$f_w = \begin{cases} 2R_W^{-1/2} & , \quad R_w < 1.15 \times 10^5 \\ 0.0521\ R_w^{-0.187}, & R_w \geq 1.15 \times 10^5 \end{cases} \qquad (25)$$

The wave Reynolds number R_w is given by

$$R_w = \frac{U_b^2 T}{2\pi\nu} \quad , \qquad (26)$$

where T is the wave period. The wave stress is calculated in the same way regardless of the presence or absence of fluid mud. The stress at the bed due to currents is found from equation (6) or (10), and the wave-current interaction term is also dependent on whether fluid mud is present. It is given by

$$\tau_{wc} = \frac{B}{4}\,(ff_w)^{1/2}\ U_b|U|\rho_w \quad ,$$

(27)

where B is a dimensionless quantity whose value depends on the relative direction of waves and current. At present, the model takes no account of wave direction so an average value is chosen, namely $B = 0.3594$, as recommended by Soulsby (Ref 8). In equation (27) the current U is taken to be the water velocity, or if fluid mud is present, then the fluid mud velocity is used. Similarly, the friction factor of equation (25) is adapted for fluid mud by substituting the fluid mud viscosity as given in equation (13).

As explained in Chapter 2, it is assumed that in the presence of waves the thickness of the fluid mud layer is not less than the wave boundary layer thickness. There is also a maximum concentration for the fluid mud, defined by the model input parameter c_0. These two considerations uniquely fix the concentration and depth of the fluid mud layer. In the early stages of the fluidisation process, or if the availability of weak mud on the bed is limited, the fluid mud concentration will be less than c_0. Once sufficient mud has been fluidised for the concentration to reach c_0, further fluidisation causes the depth of the layer to increase with no change in the concentration.

The wave boundary layer thickness is given by

$$\delta = \left(\frac{f_w}{2}\right)^{1/2} \frac{U_b T}{2\pi} \quad , \tag{28}$$

where f_w, the wave friction factor is calculated using the concentration-dependent viscosity of the fluid mud, so that denser fluid mud yields a thicker boundary layer.

The wave orbital velocity is compared with a threshold value, which corresponds to a wave height equal to 70% of the local depth. If it exceeds this threshold, the wave is assumed to be breaking, thus generating turbulence throughout the water column. In this situation any mud in the fluid mud layer is transferred into suspension and the thickness of the fluid mud layer is set to zero.

4 Finite difference representations of the mud transport equation

4.1 Transport of suspended mud

As with the existing MUDFLOW-2D program, the transport of suspended mud, given by equation (1), is calculated using explicit upstream differences. The flux of suspended mud in the x-direction, F_x, is given by

$$F_{xij}^{n+1/2} = \begin{cases} U_{ij}^{n+1/2}\, \Delta t \Delta y\, C_{ij}^{n} d^{n} \quad , & U_{ij}^{n+1/2} \geq 0 \\ U_{ij}^{n+1/2}\, \Delta t \Delta y\, C_{i+1j}^{n} d^{n} \quad , & U_{ij}^{n+1/2} \leq 0 \end{cases} \tag{29}$$

In this notation, the superscript denotes the time-step number and the subscripts are row and column numbers. d is the water depth, Δt is the duration of a time-step and Δy is the grid spacing in the y-direction. The calculation of the flux in the y-direction is similar. The new concentration is then

$$C_{ij}^{n+1} = C_{ij}^{n} + \frac{1}{(\Delta u \Delta y d^{n+1})} \left[F_{xi-1j}^{n+1/2} + F_{yij}^{n+1/2} - F_{yij-1}^{n+1/2} - F_{xij}^{n+1/2}\right] + \mathit{sources} - \mathit{sinks} \tag{30}$$

Note the sign convention used, that the row counter, *i*, increases in the negative y-direction, whereas the column counter, *j* increases in the positive x-direction.

4.2 Fluid mud flow

The velocity of the fluid mud is calculated in a partially implicit way, as follows:

$$U^{n+1/2}_{mij} = \frac{U^{n-1/2}_{mij} - slopeterms - \Omega V^{n-1/2}_{mij} + \frac{\Delta t}{d_m \rho_m}\tau_i' U^{n-1/2}_{mij}}{1 + \frac{\Delta t}{d_m \rho_m}(\tau_o' + \tau_i')} \qquad (31)$$

where τ_o is the bed stress τ_o divided by the modulus of the fluid mud velocity and τ_i is the interface stress τ_i divided by ΔU. Other symbols are as used previously. The expression for the momentum in the y-direction is similar, but differs because of the sign convention mentioned above.

The flux of fluid mud through the face of each cell is then calculated by

$$F^{n+1/2}_{xij} = \begin{cases} U^{n+1/2}_{ij}\, \Delta t \Delta y\, C^n_{ij} d^n, & U^{n+1/2}_{ij} \geq o \\ U^{n+1/2}_{ij}\, \Delta t \Delta y\, C^n_{i+1j} d^n, & U^{n+1/2}_{ij} \leq o \end{cases} \qquad (32)$$

The calculation of the depth of fluid mud in each cell depends on the wave boundary layer thickness, δ, in that cell and on the total mass of mud per m^2 of the cell, M. We have

$$M = d^n_{mij} C^n_{mij} - F^{n+1/2}_{mxij} + F^{n+1/2}_{mxi-1j} - F^{n+1/2}_{myij} + F^{n+1/2}_{myij-1} + sources - sinks \qquad (33)$$

and if M is greater than δ multiplied by c_0 we use

$$d_m = \frac{M}{C_o} \qquad C_m = C_o \qquad (34)$$

otherwise,

$$d_m = \delta \qquad c_m = \frac{M}{\delta} \qquad (35)$$

4.3 Mud exchange between layers

The equations for the sources and sinks of mud via erosion, settling, entrainment, dewatering and bed consolidation are represented by first order forward differences in time, using the corresponding differential equations given in section 3.4.

5 Application of the model to a test case

5.1 Background

The test case chosen for the study was Tees Bay. A pilot model of mud transport was set up to test the new modelling approach, based on flow results from a previous HR study of the area (Ref 11). The model used a 125m grid extending approximately 9km offshore and 14km along the coast. The grid was aligned with a straight dredged channel in the approach to the harbour (see Figure 2). The boundary conditions for the flow model were based on a mean spring tide with a range of 4.6m.

The aim of the study was to assess the effects of a storm on bed deposits. To obtain initial conditions for the storm study with reasonably large deposits, the following procedure (which was not intended to be realistic) was followed. The model was run from a cold start with no bed deposits but a high concentration of suspended mud (1000ppm). To allow this mud to settle onto the bed and give time for the bed to consolidate, 8 tides were run with no waves. No fluid mud formed during this period. Before running the storm conditions, any remaining mud in suspension was artificially removed. This produced a pattern of bed deposits which differs from the actual physical conditions in that no sand is present in the model, whereas in Tees Bay itself the bed has large sandy areas.

The storm waves were based on observations of the storm of 6th - 10th February 1983. The significant wave height was 5m and the zero crossing period was 7.6 seconds. The pattern of wave orbital velocities was produced by the HR PORTRAY model, averaging over three incident wave directions: 10 degrees, 25 degrees and 40 degrees North. The duration of the modelled storm was 12 hours, beginning at high water.

5.2 Mud properties

A variety of properties of mud in suspension, fluid mud and the muddy bed are input to the model at run time, to allow for the fact that mud from different geographical locations can often have quite different properties. These parameters must be determined from field or laboratory measurements, given in this case by Ref 6 and Ref 12.

<u>Settling</u>

Minimum settling velocity, V_{min} = 0.0001 m/s
Settling constant, R_0 = 0.0002 $m^4/kg/s$

Ratio of concentration at the bed to depth averaged concentration, beta = 2.0

Fluid mud

Maximum concentration, c_0 = 75 kg/m^3
Mud viscosity at maximum concentration, $\upsilon_m(c_0)$ = 0.00066 m^2/s
Dewatering velocity, V_0 = 0.00005 m/s

Bed

Consolidation rate A = 0.00003 s^{-1} ~ 1/(10hrs)
Number of bed layers = 5
Erosion shear stress, (N/m^2)
layer 1 : 0.2
layer 2 : 0.35
layer 3 : 0.62
layer 4 : 0.8
layer 5 : 1.0
Yield strength, (kg/m^2)
layer 1 : 0.38
layer 2 : 2.78
layer 3 : 10.53
layer 4 : 85.0
layer 5 : infinity

5.3 Results

The results of the simulation are illustrated in figures 3 - 15. For figures 3 - 10, two moments in time during the storm have been chosen for plots: six hours after the start of the storm, which is a few minutes before low water (LW) and twelve hours after the beginning of the storm, which is shortly before high water (HW).

When fluid mud is first formed, its depth corresponds to the thickness of the wave boundary layer, but since the mud can flow under the influence of gravity, hydrostatic pressure gradients and overlying currents, the distribution of fluid mud a few hours after its formation can be quite different (see Figures 3 and 4). Note that the bed is fluidised over most of the bay, except for very close to the coast, and a small area inside the breakwaters. Possibly the most important feature of the fluid mud distribution is that the dredged channel has a relatively deep layer of fluid mud: 40-60 cm compared to 5-20 cm over much of the bay. This is due primarily to mud flowing into the trench from either side, as can be seen from plots of the fluid mud velocity (Figures 5 and 6). Consideration of the bed contours in figure 2 shows that the mud is flowing down the slope into the trench, but is also influenced by the tidal currents (Figures 7 and 8). At low water the current flows north-west along the coast, so the largest fluid mud velocities are on the south-eastern slope of the trench; at high water the current is reversed and the fluid mud on the north-western slope is moving into the trench more quickly. There is a small mud current along the bottom of the trench, directed away from the coast.

Figures 9 and 10 illustrate the concentration of suspended mud during the storm. In figure 9, the patches of high concentration near the beach are due to breaking waves. As explained in Chapter 2, if the wave height exceeds 70% of the depth, the waves are judged to be breaking and any fluid mud is then distributed through the whole water column. Elsewhere, the suspended concentrations are low, less than 100 ppm over most of the model area and no higher than 200 ppm anywhere. These values are smaller than the observed concentrations (Ref 11) which can exceed 600ppm during storms. This illustrates a possible inaccuracy in the representation of the entrainment of fluid mud by overlying water currents: in the model the mud tends to be trapped too strongly in the fluid mud layer.

This effect could also limit the mobility of mud during the storm, as the fluid mud moves more slowly than the tidal currents.

Figure 11 shows the net erosion and deposition of mud caused by the storm, calculated by comparing the total bed deposits immediately before the start of the storm with those three tidal periods after the end of the storm, allowing time for fluid mud to dewater after the wave activity has ceased. The general pattern is one of erosion along the coast except in the dredged channel, where considerable net deposition occurs. Further from the coast, there are patches of erosion and deposition, caused by local bathymetry features. The wave orbital velocities are large in the shallower regions closer to the coast, leading to considerable erosion of the bed into fluid mud, which subsequently flows either into the channel or away from the coast, moving downhill or being swept along by the tidal currents. There is little change in the bed situation within the breakwaters as comparatively little fluid mud is formed in this area and the tidal currents are not sufficiently strong to drive fluid mud up the bed slope into the harbour.

Figures 12 - 15 give time histories over the period of the storm of fluid mud depth, total bed deposits, suspended mud concentration and fluid mud concentration at seven points, the locations of which are shown in figure 2. Positions 3, 4 and 5 are in the dredged channel.

At position 1, the upper part of the bed is fluidised as the storm begins, causing a sudden decrease in bed deposits. As the storm continues, the bed undergoes a small degree of further erosion, but as the fluid mud depth remains approximately constant, this must be balanced by net outflow of fluid mud from that cell, or entrainment by tidal currents. In the last two hours of the storm, the rapid increase in suspended mud concentration may be partly due to entrainment, but from comparison with figures 9 and 10, seems more likely to be caused by advection of mud by the tidal currents, with the majority of the entrainment occurring further north.

At position 2, all of the mud on the bed is quickly eroded when the storm begins, but thereafter the amount of fluid mud steadily decreases, by a combination of entrainment and fluid mud flow. Position 3 shows similar behaviour to position 1, except that in the first half of the storm there seems to be a net inflow of fluid mud, as would be expected from the fact that position 3 is in the dredged channel. This effect is more pronounced at station 4, where a considerable quantity of fluid mud flows into the channel from either side. The last data point on the graph (at 12.42 hours after HW) is shortly after the end of the storm, and in the absence of waves, the fluid mud begins to dewater, causing the upturn in the bed deposits curve. Three tidal periods after the end of the storm, net deposition caused by the storm is in the region of 200 kg/m^2 in a small area around station 4, mainly due to the movement and subsequent dewatering of fluid mud.

Position 5 shows a considerable increase in bed deposits during the course of the storm. During the early stages of the storm, a considerable amount of fluid mud flows into this part of the channel from either side. This causes an attenuation of the wave induced stress at the bed, because the fluid mud layer is much thicker than the wave boundary layer (see section 3.3). As the water is relatively deep here, the wave orbital velocity is only moderate. If the fluid mud is also moving very slowly, then the stress at the bed can be sufficiently low for dewatering to occur. This is the case at position 5, between three and six hours after the start of the storm.

Position 6 shows similar behaviour to position 1. At position 7, all of the bed deposits are fluidised as the storm begins. The tidal currents cause entrainment of the fluid mud, which decreases the concentration of the fluid mud layer, as its thickness is governed by the wave boundary layer thickness. In the latter stages of the storm, the reduction in mud concentration in the wave boundary layer causes its thickness to decrease, as explained in section 3.5.

The main finding of the modelling exercise is that sediment transport during a storm can be strongly influenced by the movement of fluid mud, particularly in areas where there are steep bed slopes, as with the dredged channel in Tees Bay.

6 Discussion

The main processes simulated by the model are:

* Fluidisation of a muddy bed by wave action, leading to a large amount of mobile sediment in storm conditions.
* Movement of fluid mud down bed slopes under the influence of gravity, leading to high siltation rates in deep channels or pools.
* Entrainment of fluid mud by tidal currents, leading to more rapid transport of mud released from the bed by fluidisation. Although comparatively little entrainment occurs in the Tees Bay simulation, where the tidal currents are weak, other tests of the model show that entrainment is an important consideration, for example in the Severn estuary where tidal currents are very strong with a correspondingly high level of turbulent energy.
* Consolidation of the bed, allowing newer deposits to be more easily eroded than older ones.
* Slow dewatering of fluid mud in slack water conditions.
* At present, only one set of wave orbital velocities are read by the program, calculated by a wave model at a single mean sea level. Thus the variation of wave-induced bed stresses with varying water levels is not represented by the model. This could be rectified by reading several sets of wave data or modifying a single set according to instantaneous water depth.

* The effect of waves is modelled only in relation to fluidisation of the bed: no account is taken of mass transport by waves.
* The representation of the bed fluidisation process could be improved by more detailed knowledge of the influential factors. Also, better knowledge of the attenuation of wave-induced bed stress by the fluid mud layer would allow the present ad hoc assumption to be improved upon.
* The turbulent processes at the fluid mud - water interface are not fully understood. Further work, perhaps using a 1DV model of the turbulent flow, could lead to a more accurate representation of the entrainment process and its relationship to the fluid mud and suspended mud concentrations.
* More information on the flow properties of fluid mud at various concentrations might lead to an improved model.

7 Conclusions

A new mud transport model has been developed, incorporating both mud in suspension and fluid mud. The model was designed in particular to represent the fluidisation of mud by waves and has a multi-layer representation of the bed with consolidation effects.

Simulation of a storm in Tees Bay confirms that mud fluidised by waves can make an important contribution to mud transport, leading for instance to high siltation rates in a dredged channel.

The model represents the most important processes of mud transport by waves and currents. Although the scarcity of field measurements of fluid mud makes it difficult to assess quantitatively the accuracy of the model, it is clear that it gives qualitatively realistic results.

8 Acknowledgements

Mr N V M Odd is thanked for his many useful suggestions.

9 References

1. Ockenden, M.C. and Delo, E.A.
'Fluidisation of mud by waves: laboratory and field experiments'. HR Wallingford, England. Report SR268, April 1991.

2. Odd N V M, Rodger, J G.
'An analysis of the behaviour of fluid mud in estuaries'. HR Wallingford, England. Report SR84, March 1986.

3. Odd N V M, Cooper A J.
'A two-dimensional model of the movement of fluid mud in a high energy turbid estuary'. HR Wallingford, England. Report SR147, January 1988.

4. Ross, M.A. and Mehta, A.J.
'Fluidisation of soft estuarine mud by waves' in 'The microstructure of fine-grained sediments: from mud to shale',
R.H. Bennett (ed). Springer-Verlag, New York, 1988.

5. Jiang, F. and Mehta, A.J.
'Some observations on fluid mud response to water waves' in 'Dynamics and Exchanges in Estuaries and the Coastal Sea', D. Prandle (ed). Springer-Verlag, Berlin, 1991.

6. HR Wallingford. 'Fluid mud in estuaries'. HR Wallingford, England. Report EX2392, November, 1991.

7. Fernando H J S, Stephenson P H.
'Mixing across sheared stratified interfaces'. Environmental Hydraulics, Lee and Cheung (eds). Balkema, Rotterdam, 1991.

8. Soulsby R L.
Private communication, 1991.

9. HR Wallingford.
'The PORTRAY Harbour Wave Disturbance Model'. HR Wallingford, England. Report EX 1774, August 1988.

10. Soulsby R L, Smallman J V.
'A direct method of calculating bottom orbital velocity under waves.' HR Wallingford, England. Report SR76, February 1986.

11. HR Wallingford.
'Tees and Hartlepool Port Authority:
Dredging Review 1991'. Sir William Halcrow and Partners Ltd. and HR Wallingford, England. October 1991.

12. Ockenden M C, Delo E A.
'Dispersal of dredged material: River Tees mud properties'. HR Wallingford, England. Report SR205, March 1989.

Figures

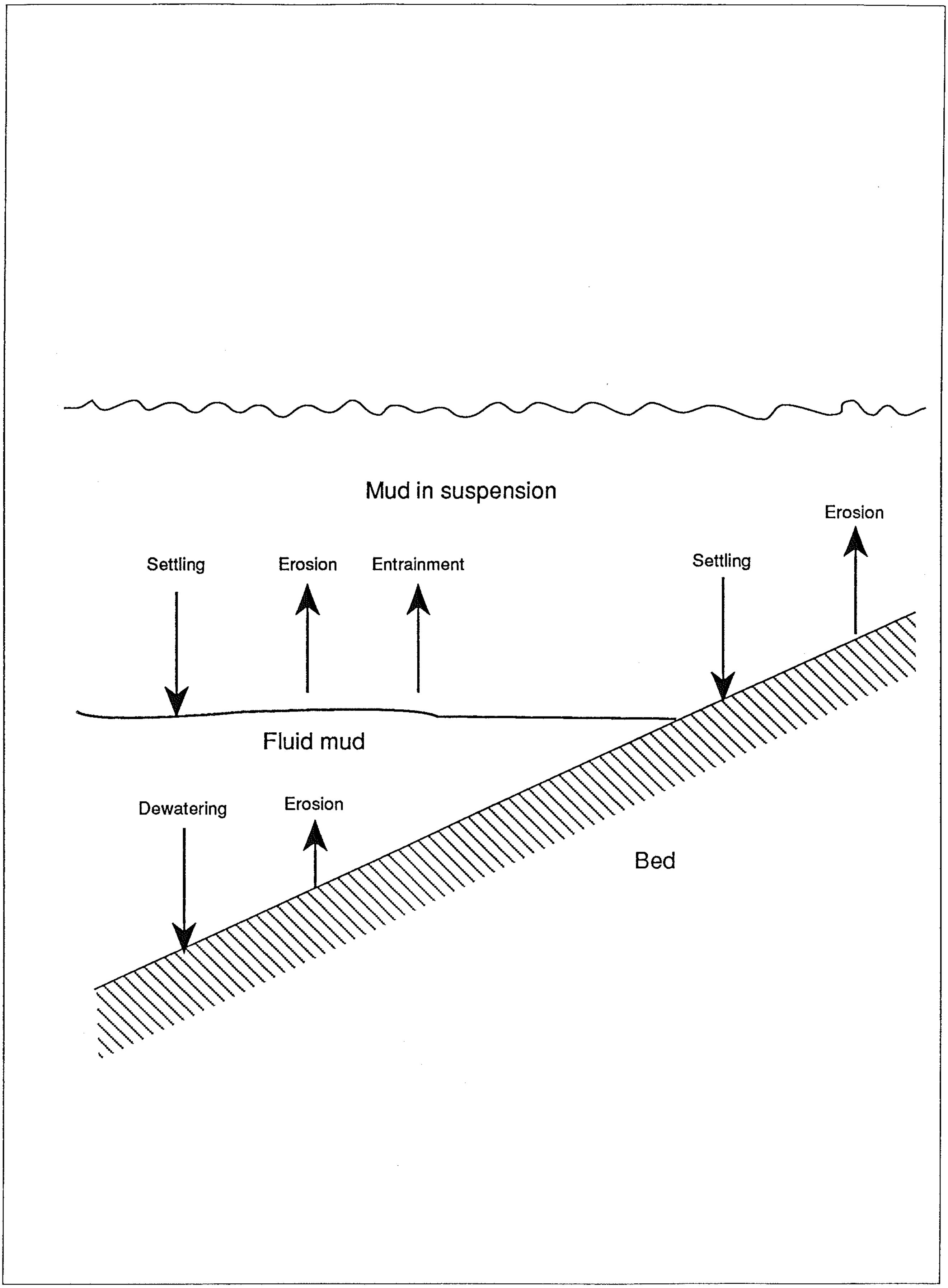

Figure 1 Mud exchange processes

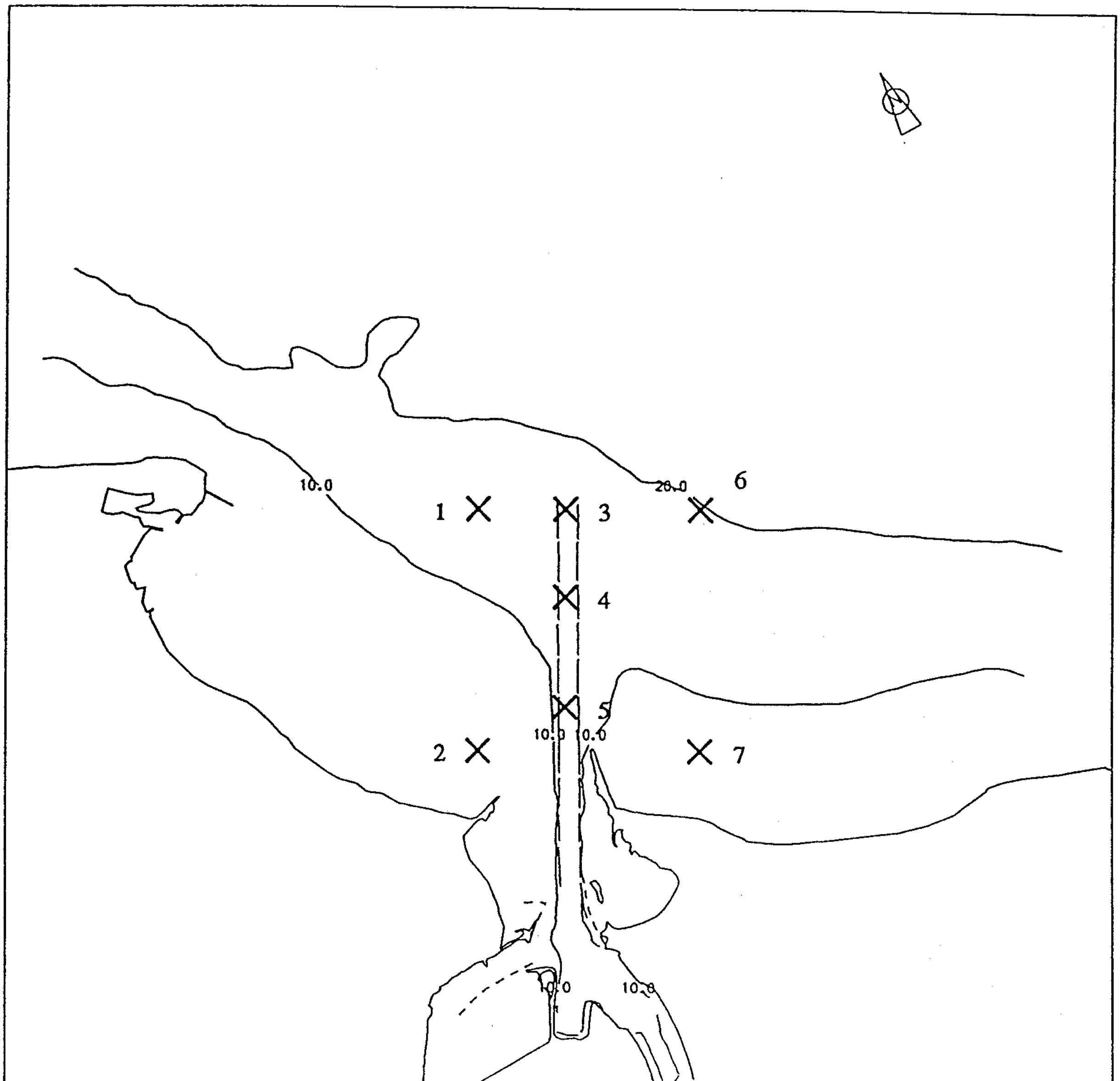

Fig 2 Location plan showing bed contours and positions for time histories

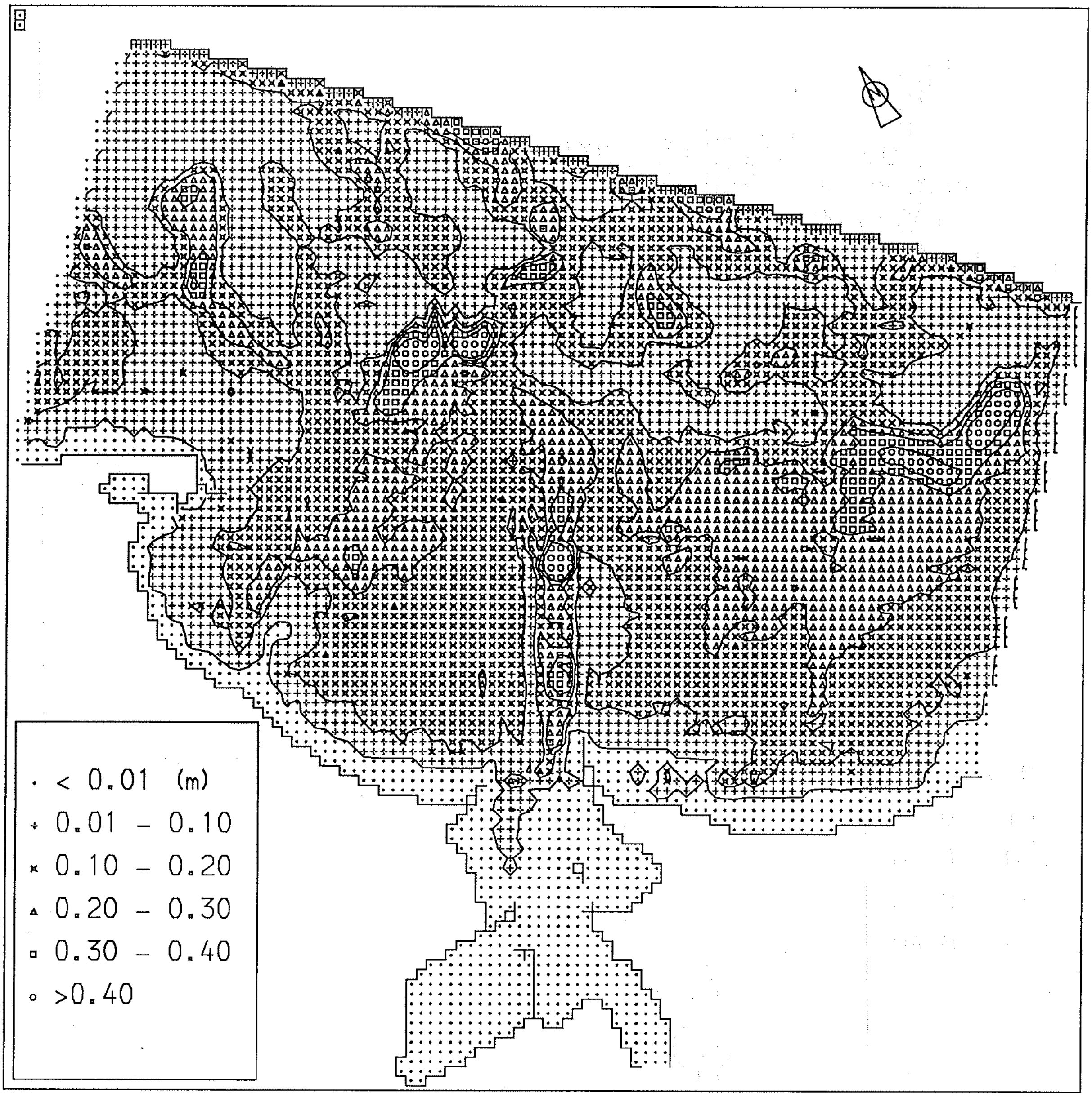

Fig 3 Fluid mud depth after 6 hours of storm waves (LW)

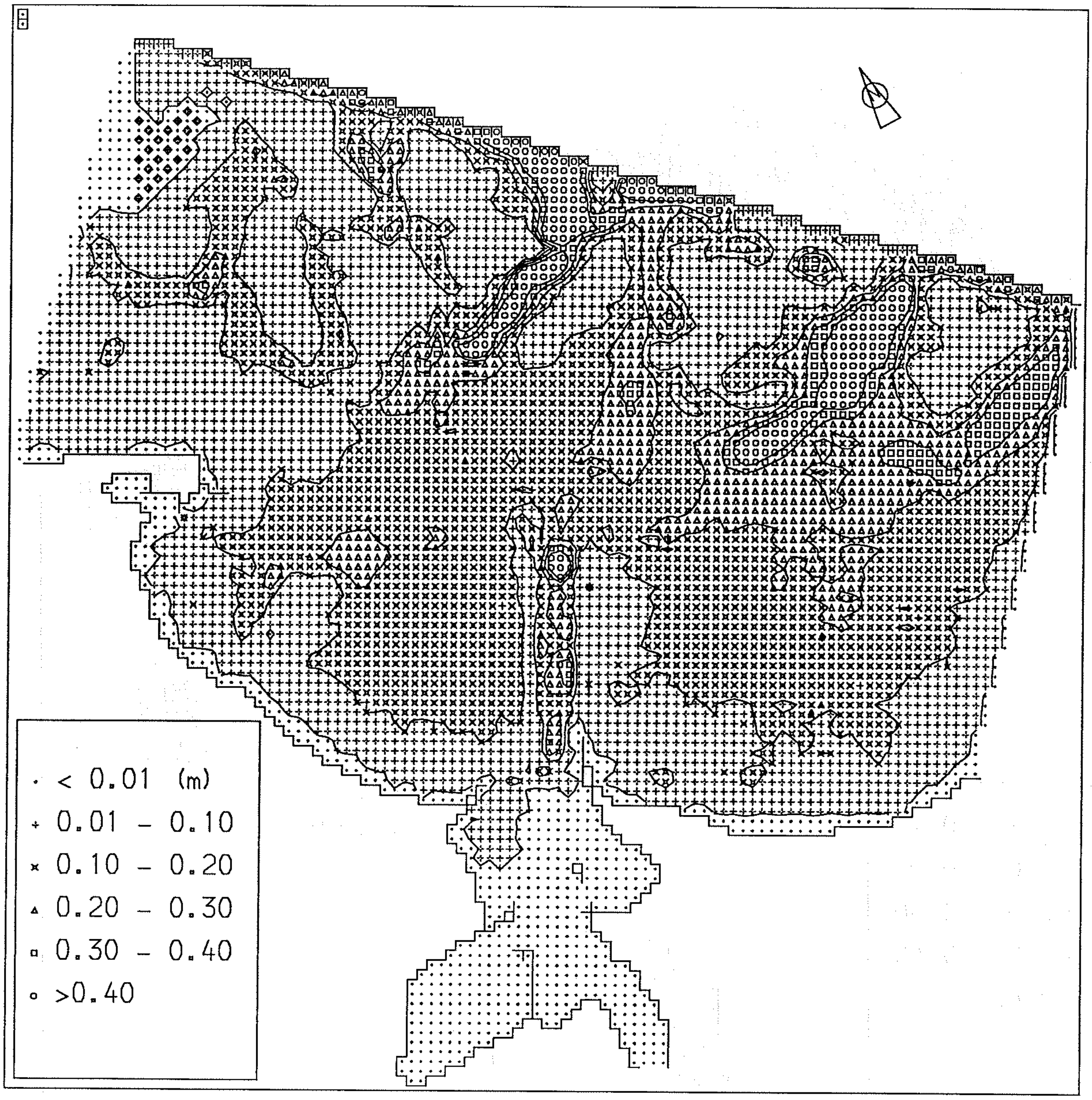

Fig 4 Fluid mud depth after 12 hours of storm waves (HW)

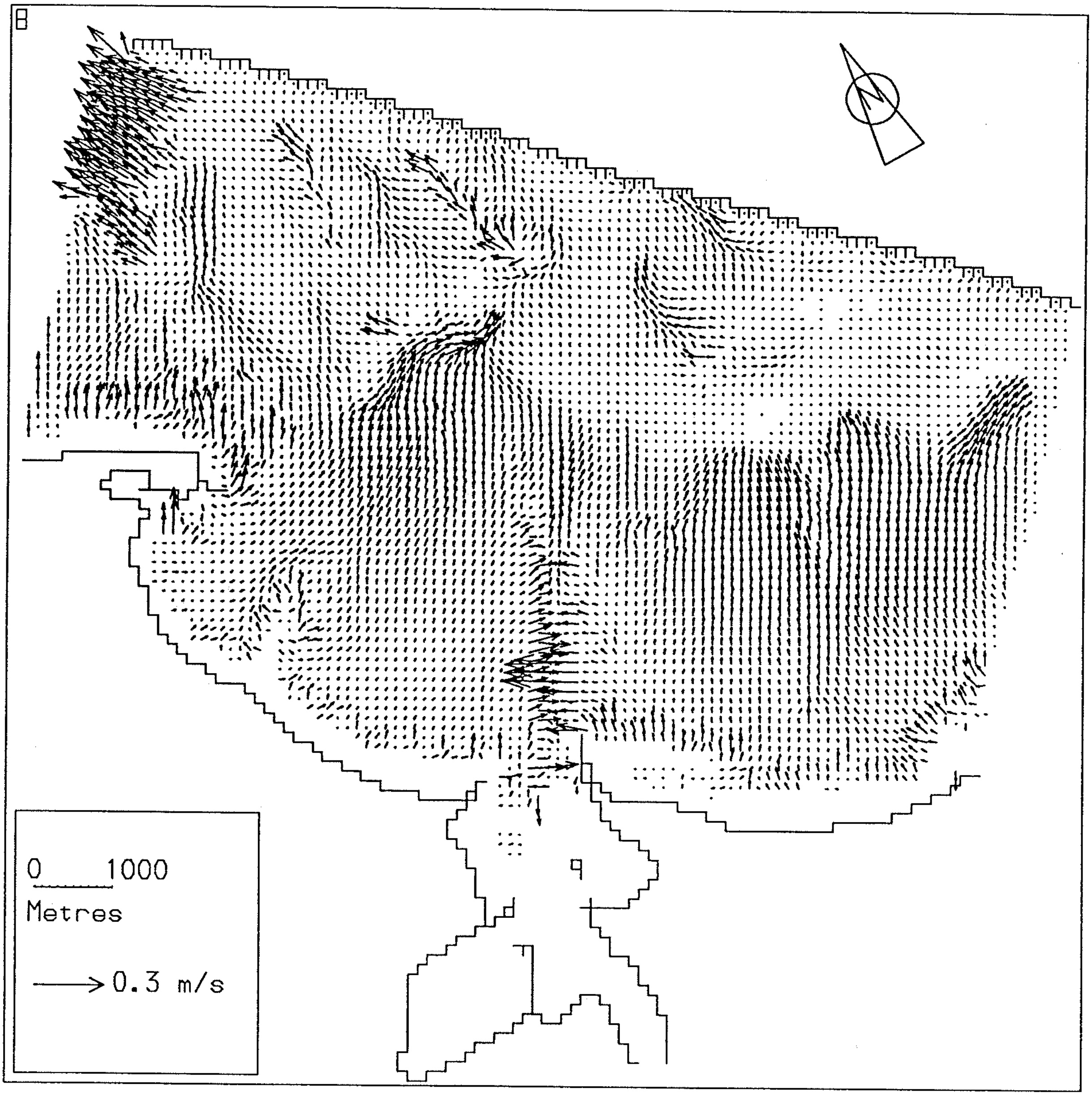

Fig 5 Fluid mud velocity after 6 hours of storm waves (LW)

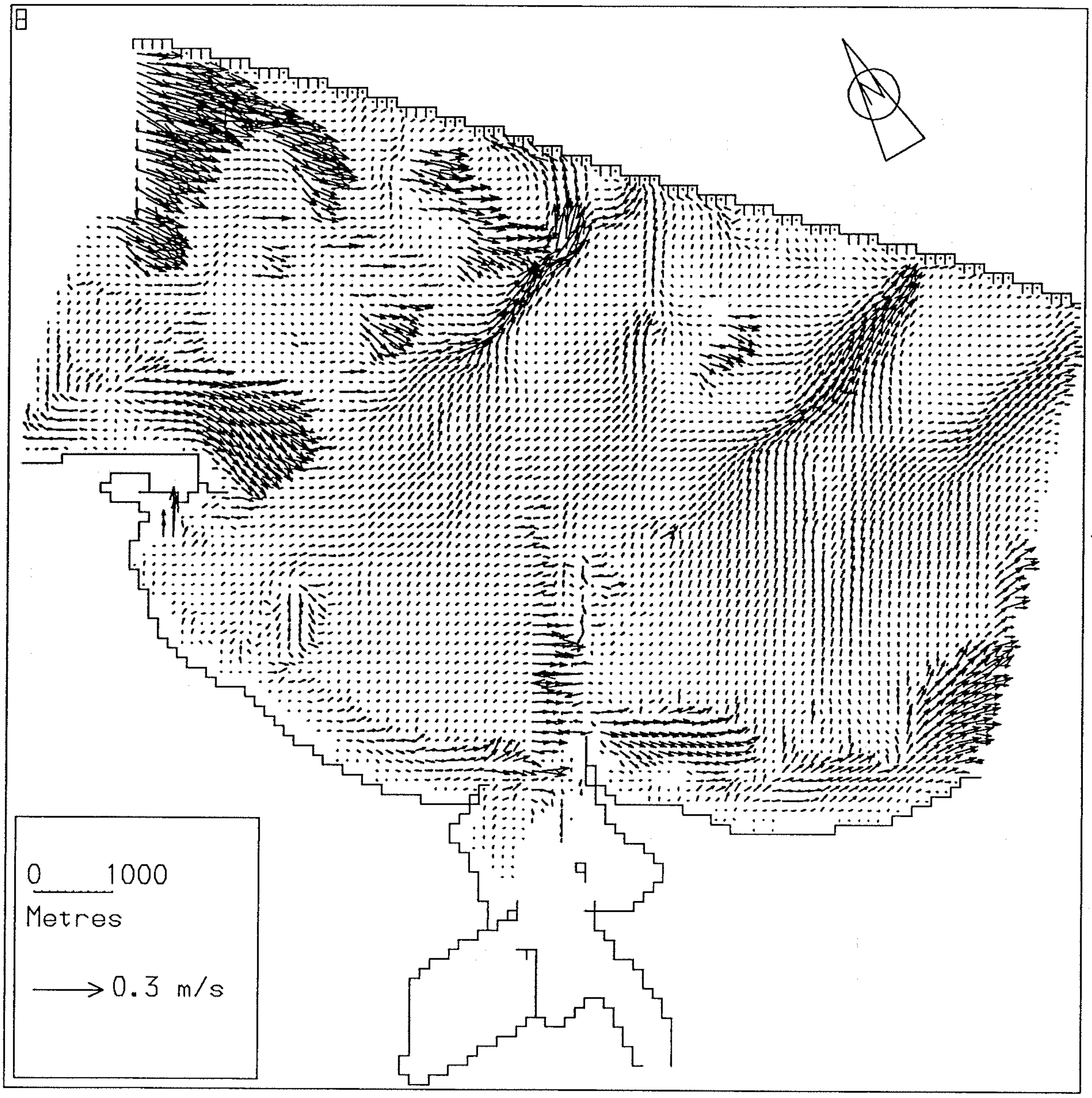

Fig 6 Fluid mud velocity after 12 hours of storm waves (HW)

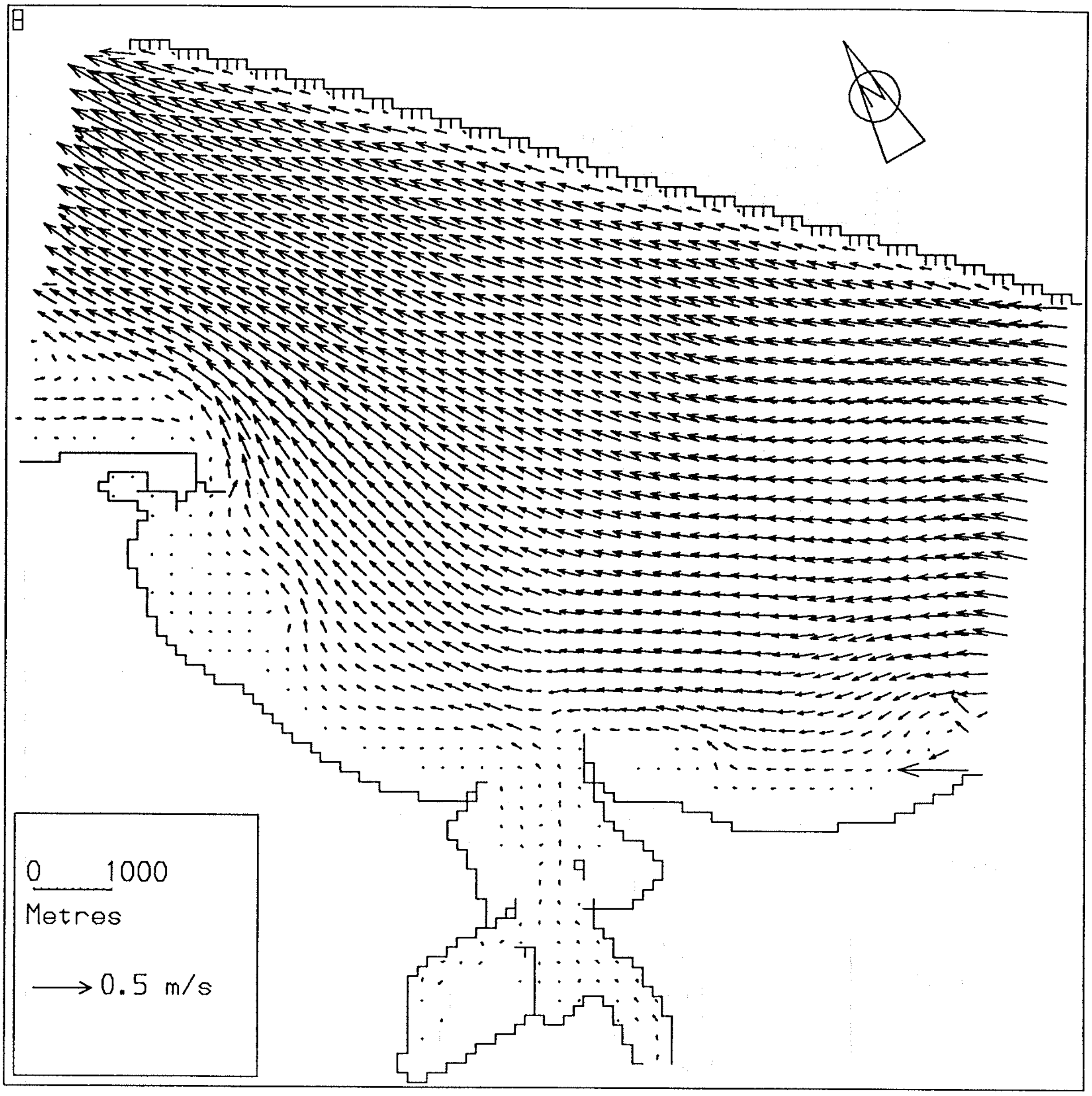

Fig 7 Flow velocity after 6 hours
of storm waves (LW)

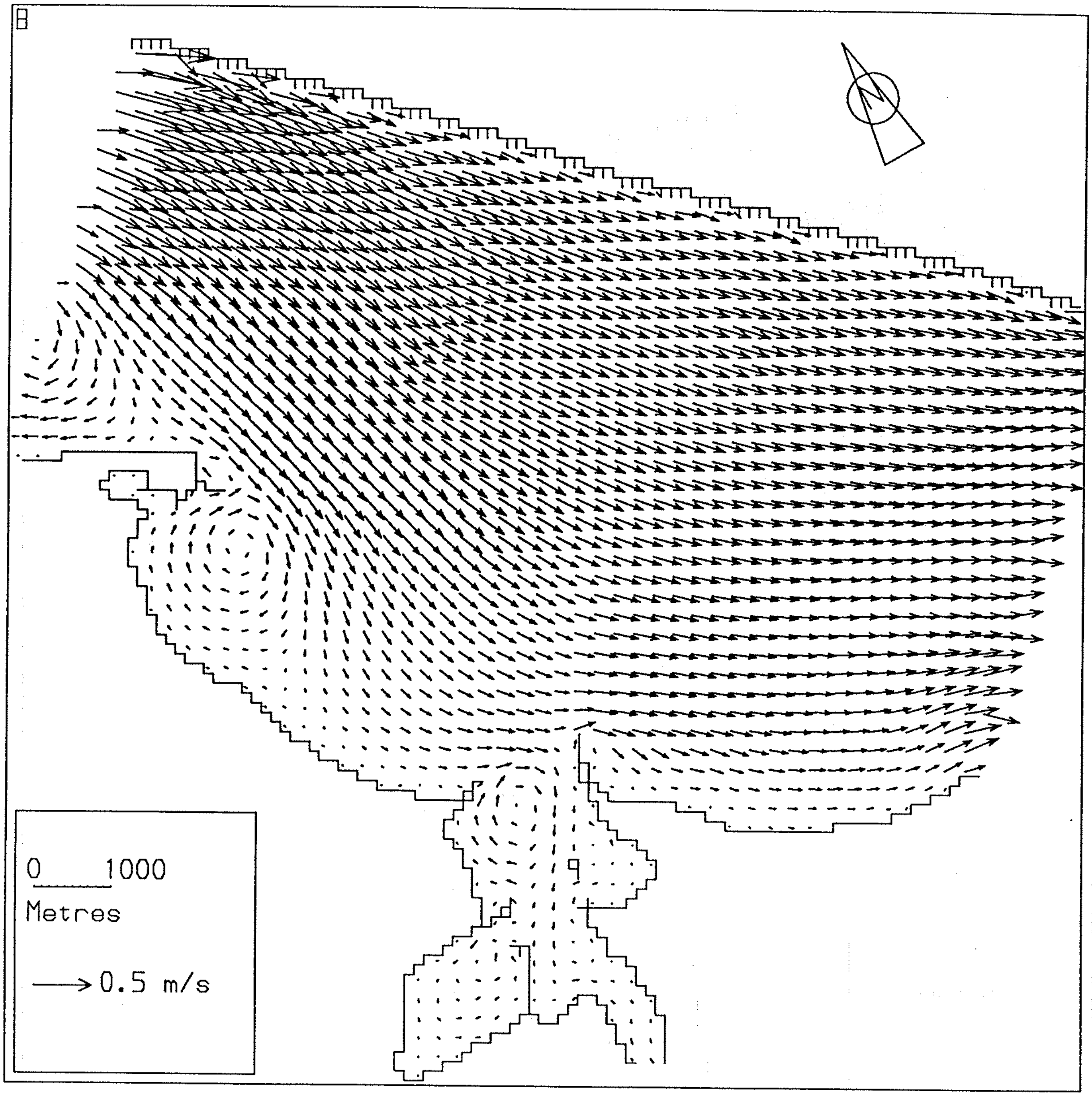

Fig 8 Flow velocity after 12 hours of storm waves (HW)

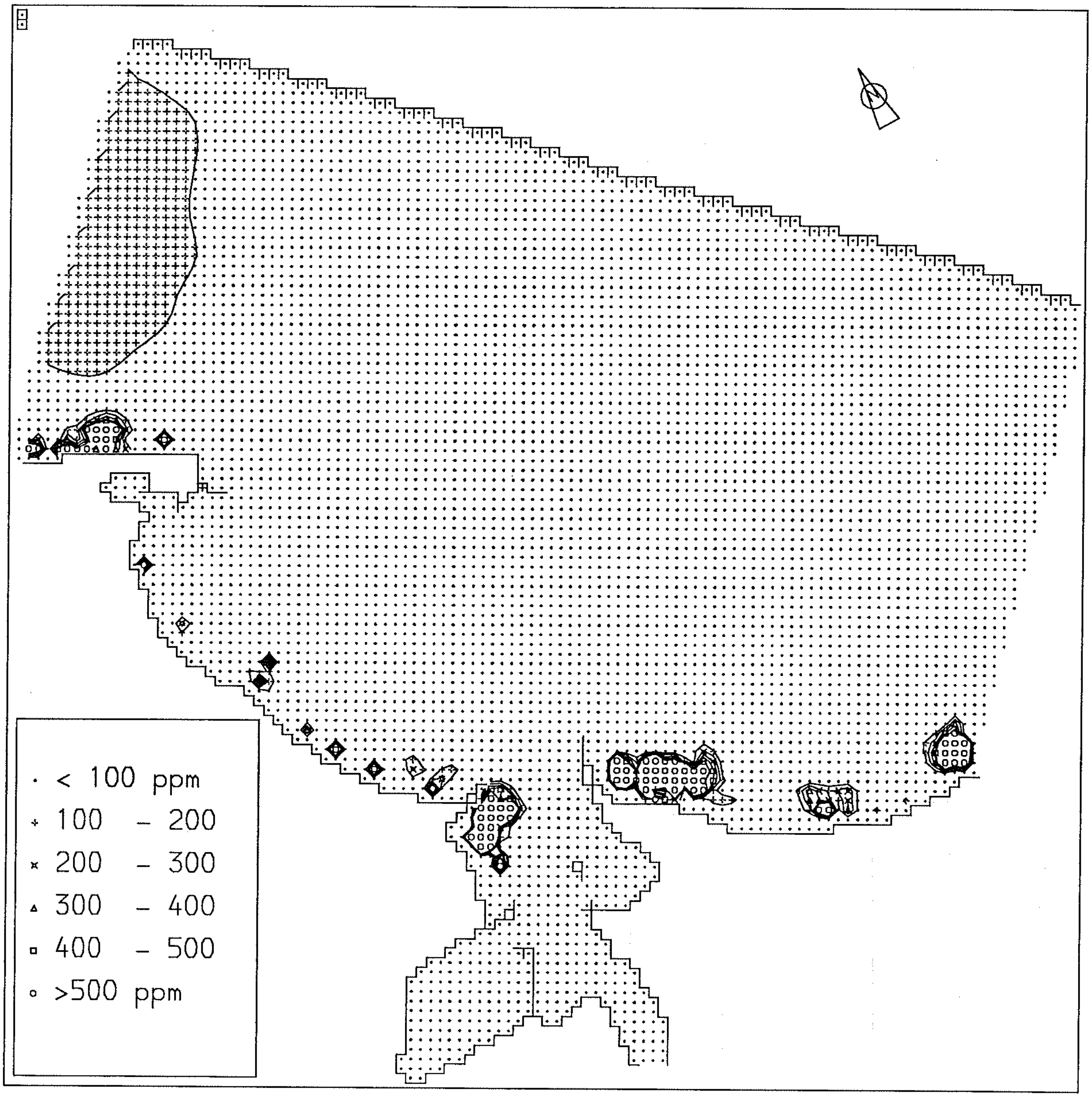

Fig 9 Concentration of suspended mud after 6 hours of storm waves (LW)

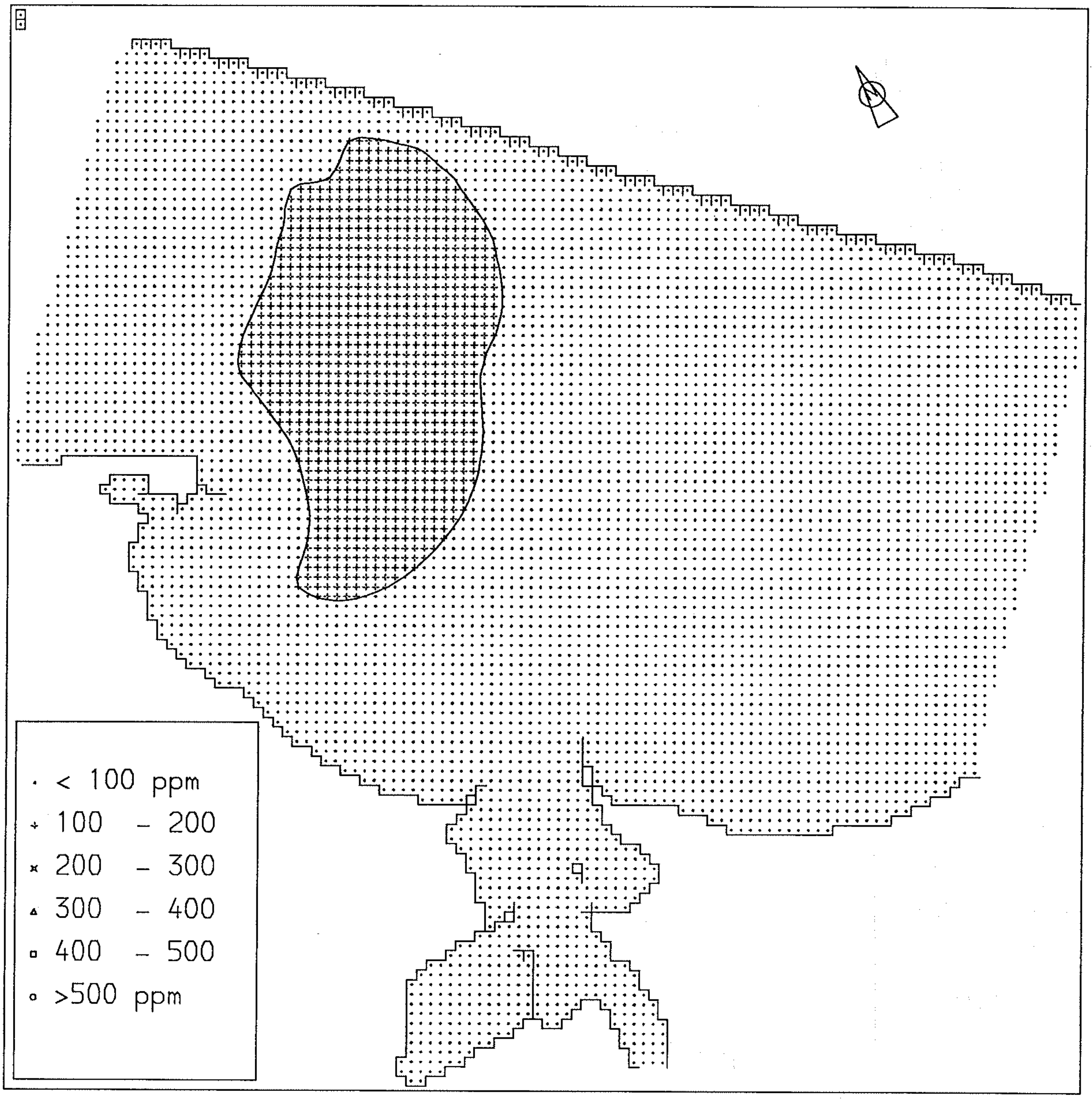

Fig 10 Concentration of suspended mud after 12 hours of storm waves (HW)

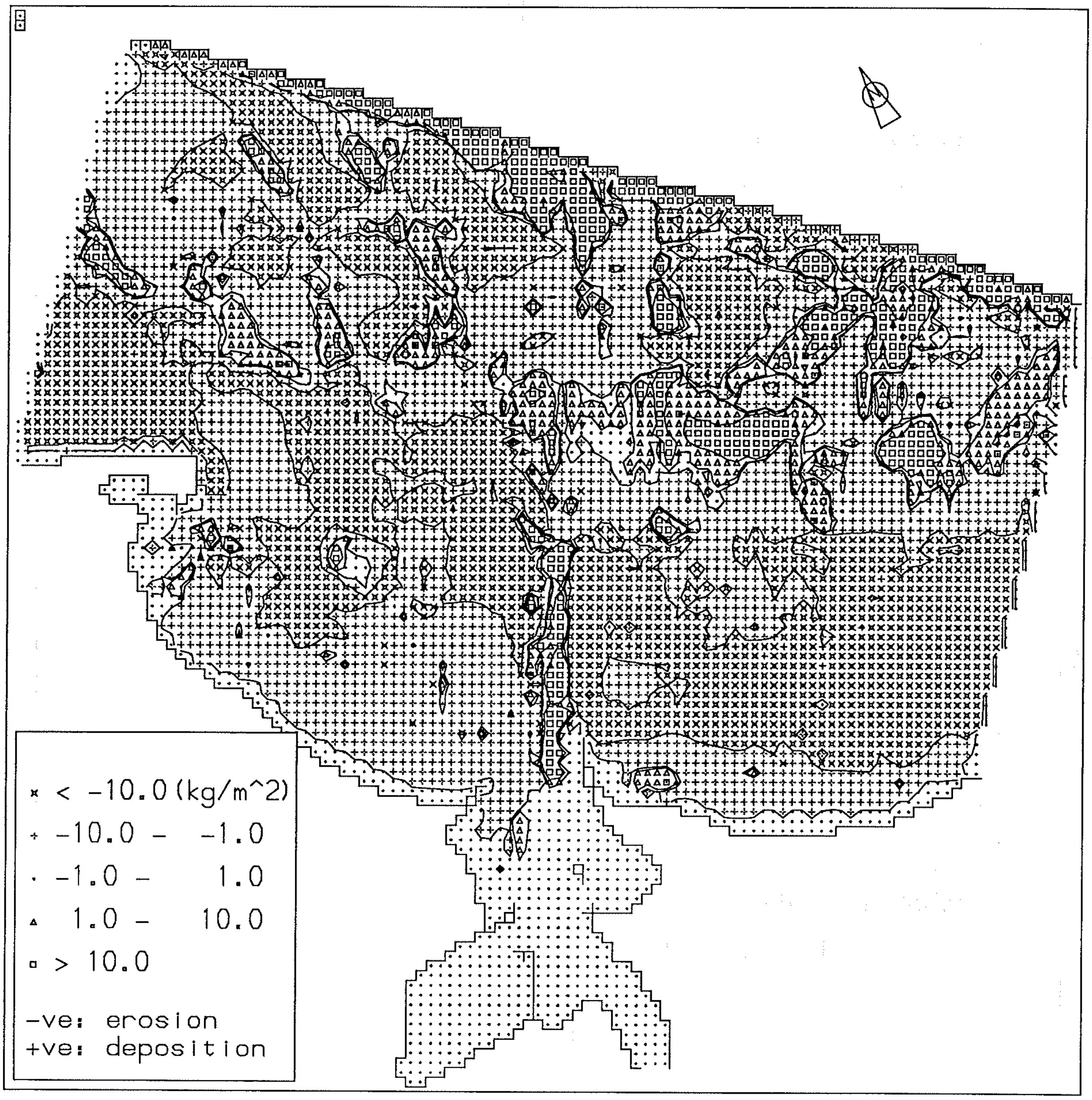

Fig 11 Net change in bed deposits resulting from a 12 hour storm

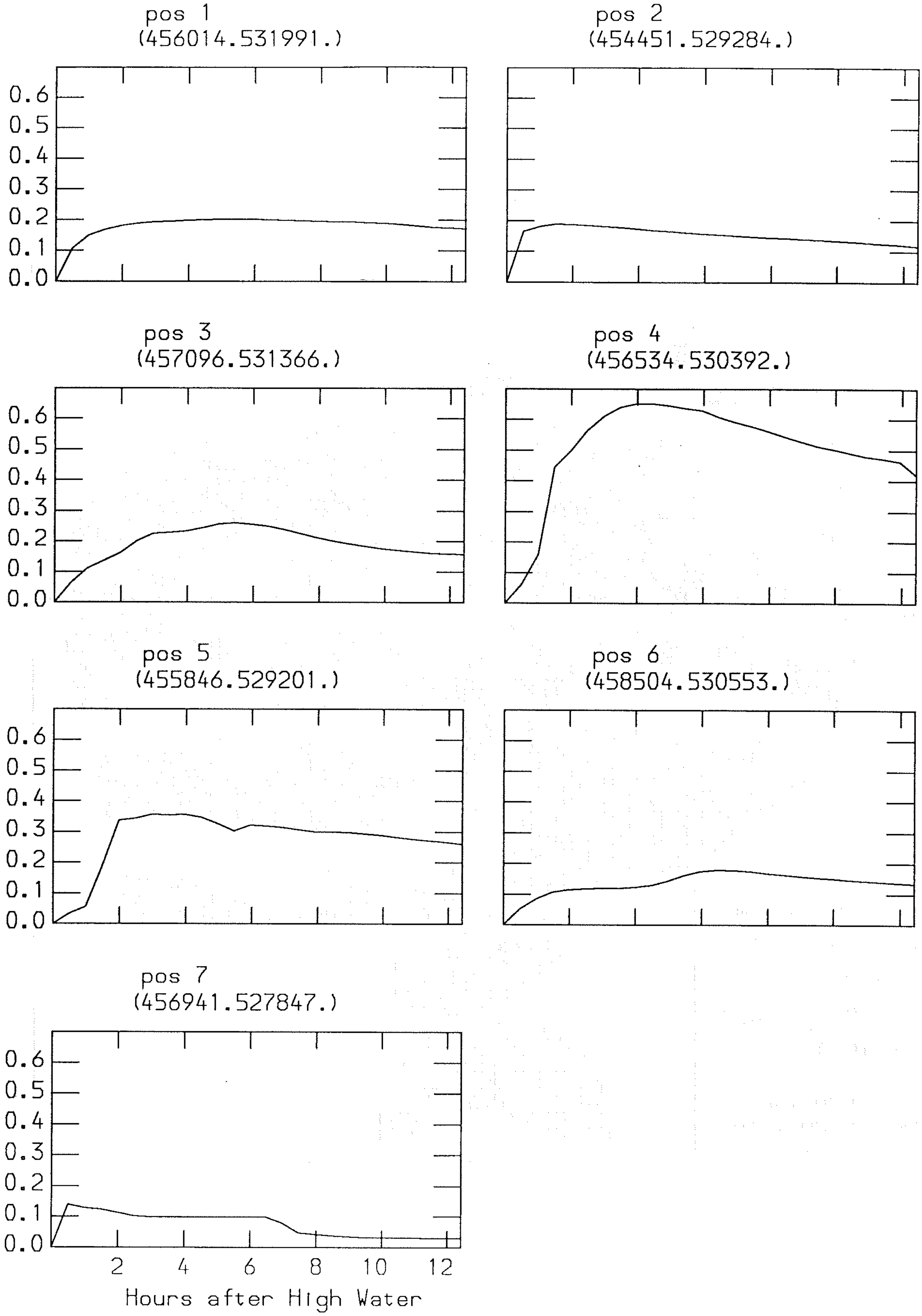

Fig 12 Fluid mud depth during storm (m)

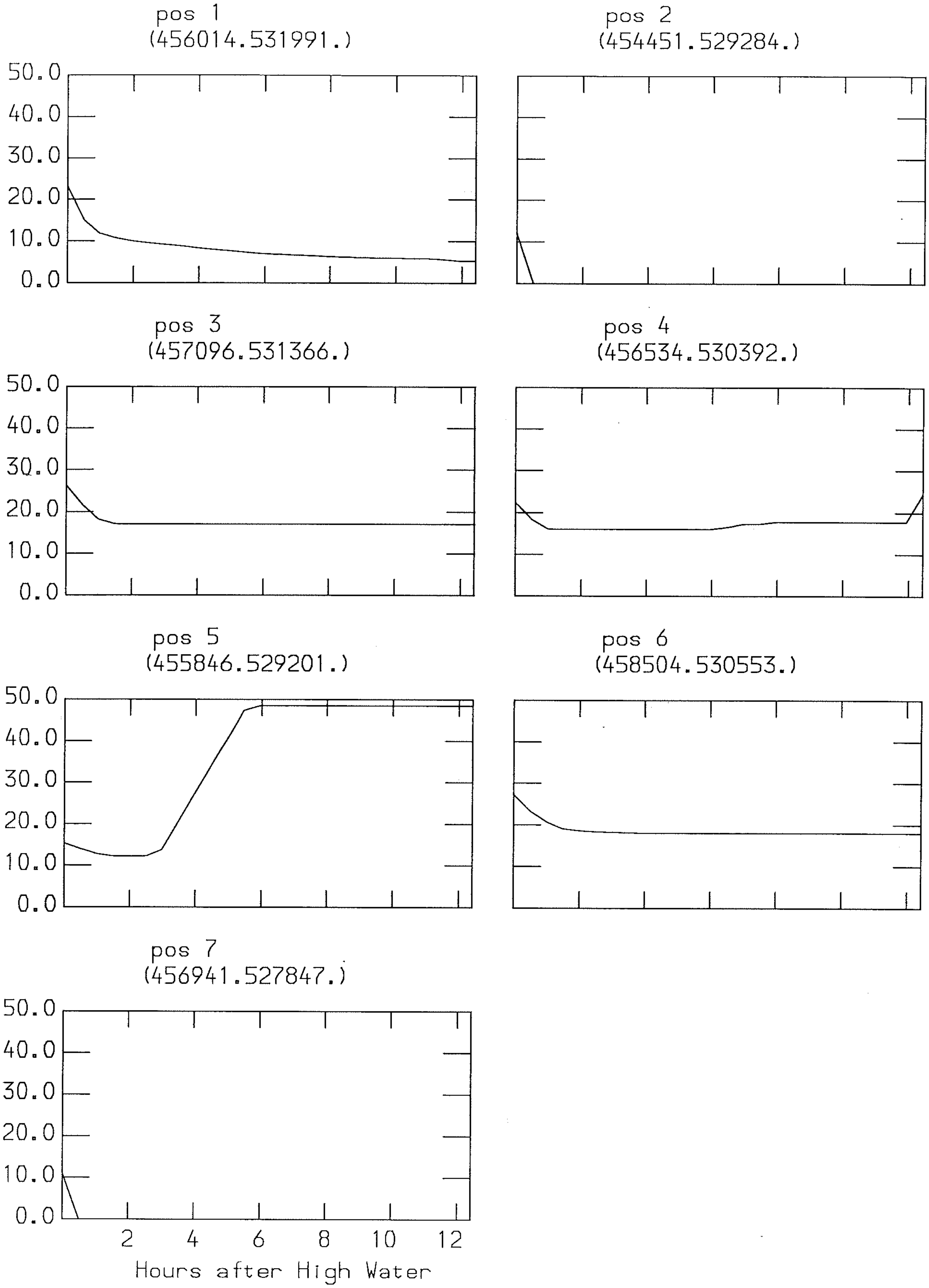

Fig 13 Total bed deposits during storm (kg/m^2)

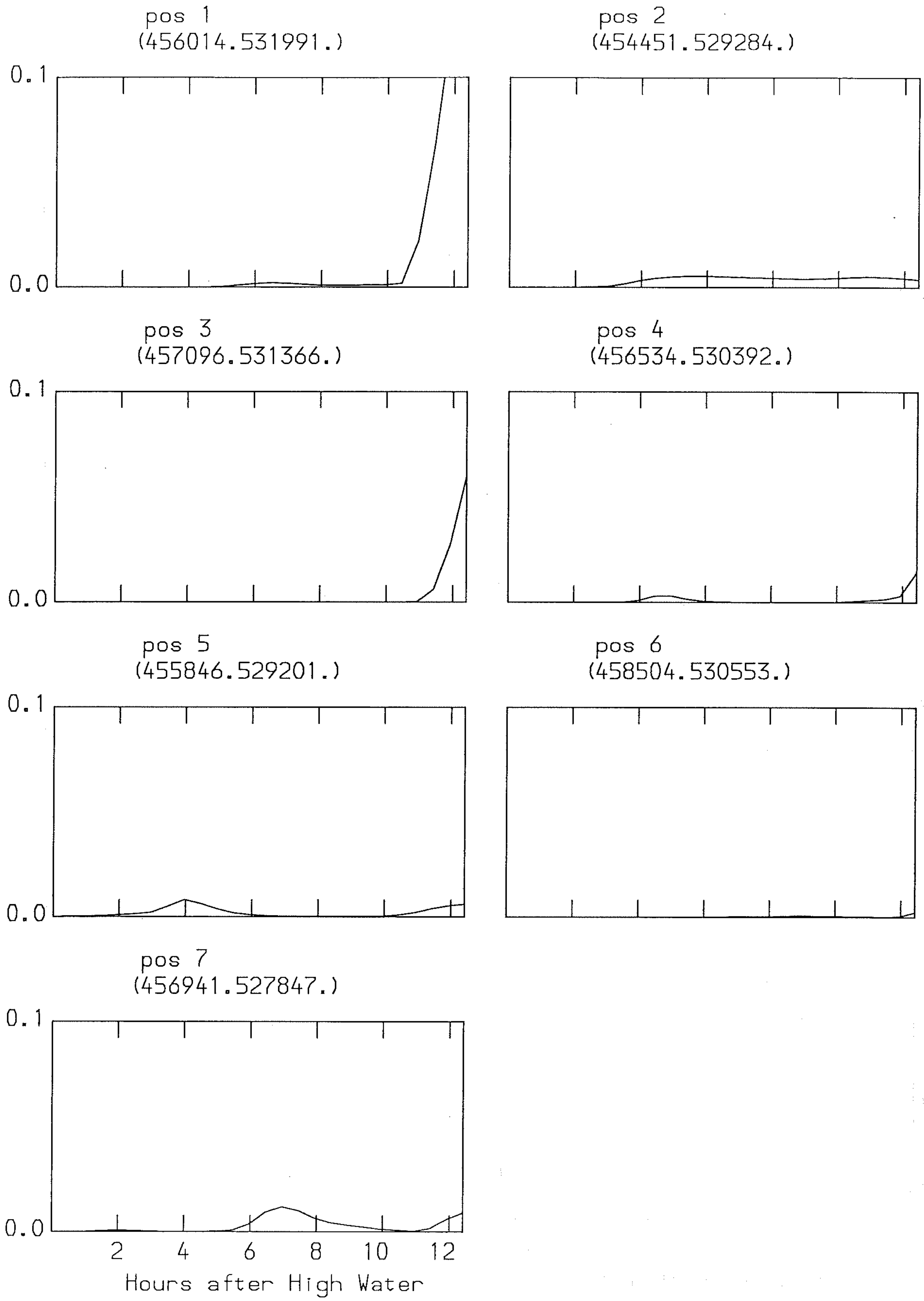

Fig 14 Suspended mud concentration during storm
(kg/m^3)

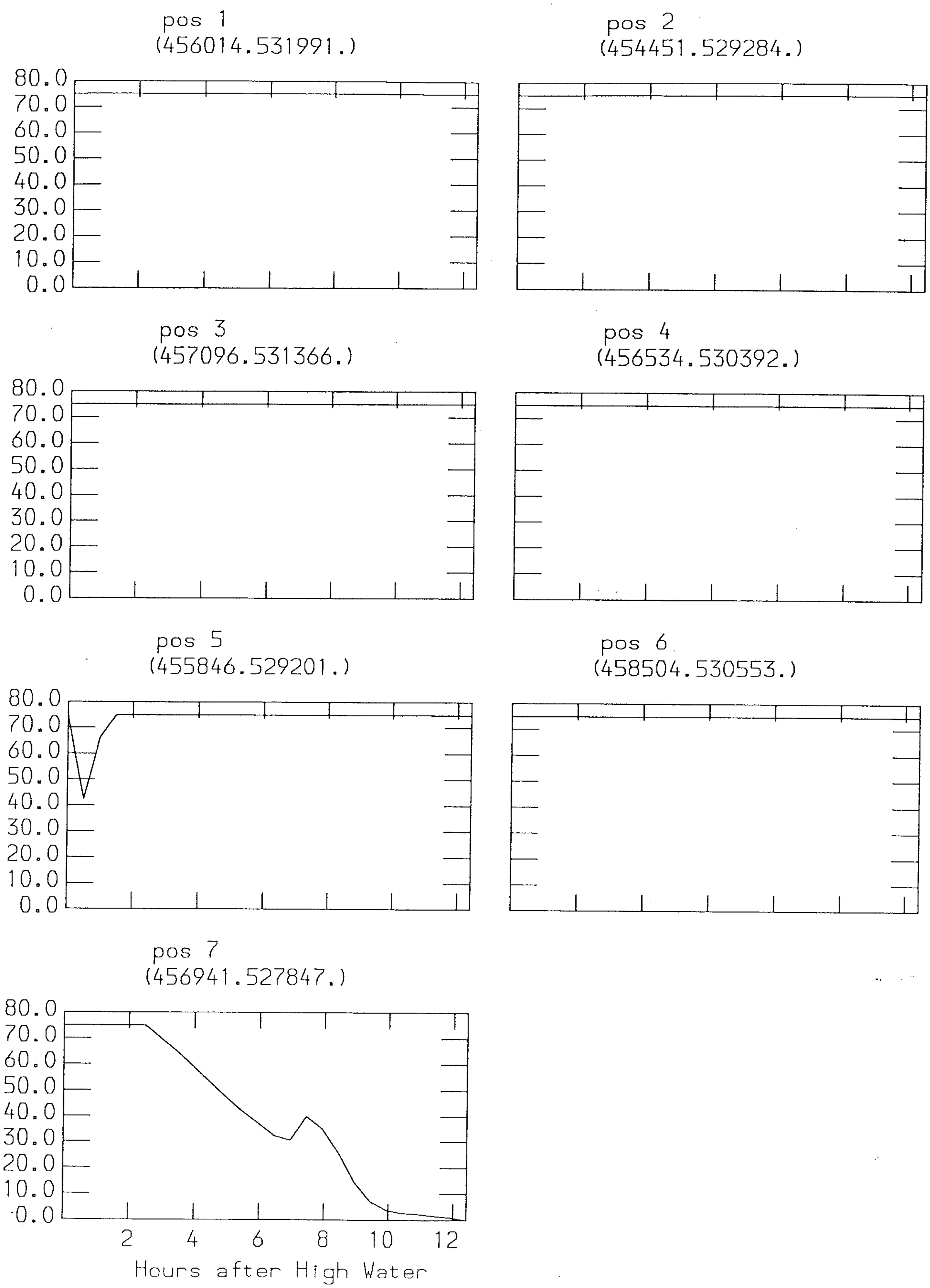

Fig 15 Fluid mud concentration during storm
(kg/m^3)